Available online at www.sciencedirect.com
ScienceDirect
Infrared Physics & Technology 51 (2008) 207–215
INFRARED PHYSICS & TECHNOLOGY
www.elsevier.com/locate/infrared

Design and characterisation of black-body sources for infrared wide-band Fourier transform spectroscopy

L. Palchetti *, G. Bianchini, F. Castagnoli

Istituto di Fisica Applicata "Nello Carrara", IFAC-CNR, Via Madonna del Piano, 10, Sesto Fiorentino, 50019 Firenze, Italy

Received 5 March 2007
Available online 28 July 2007

Abstract

The design and characterisation of small and cost-effective reference black-body sources for radiometric calibration of Fourier transform spectrometers in the mid and far infrared is presented. The paper describes the optimisation of the absorbing black-coating material and the study of two types of cavity geometry, one designed for collimated beams and one for focused beams. These two reference sources have been developed for the Radiation Explorer in the Far InfraRed spectrometer covering the 100–1400 cm^{-1} spectral range. They are currently used on-board two prototypes for ground and stratospheric balloon based atmospheric emission measurements. An emissivity of better than 0.9999 is obtained for both type of cavity geometry giving a calibration error, depending only on the temperature gradient inside the blackbody, of less than 0.5 K.

PACS: 33.20.Ea; 07.57.Ty; 44.40.+a

Keywords: Fourier transform spectra; Infrared spectroscopy; Blackbody radiation

1. Introduction

In emission spectroscopy, the calibration of the observed radiance requires the measurement of a known source of radiation, which typically is given by the emission of a blackbody (BB) cavity described by the Planck law of radiation. The design of a well-characterised and reliable BB source can be very demanding especially in which large spectral ranges and different working temperatures are required [1–3].

A BB cavity must absorb all the entering radiation in order to show an emission well-characterised by the Planck law. To approach this working condition, three requirements have the priority in the design of a BB reference source. First of all the internal absorbing surface of the cavity must have a low reflectance coefficient in the whole frequency range of interest. Secondly, the cavity geometry must maximise the number of internal reflections, and third, the temperature must be uniform and known as well as possible. Depending on the spectral range of interest and the range of temperature to be used, a BB cavity can be designed to meet the previous requirements and therefore to maximise the BB performances. We must also keep into account that in the particular case of an instrument operating on-field, for example on an aircraft or balloon platform, also limited size and weight must be added to the requirement of a reference source.

In this paper, the described requirements have been addressed for the design of two BB reference sources operating from about −10 to 120 °C in the wide spectral range of 100–4000 cm^{-1}, one to be used in a collimated beam and another to be used in a focused beam. These reference sources are required to perform the radiometric calibration of the space-borne FTS designed in the framework of the feasibility study of the Radiation Explorer in the Far InfraRed (REFIR) project [4]. The BB sources have been

* Corresponding author. Tel.: +39 055 4378540; fax: +39 055 5226311.
E-mail address: L.Palchetti@ifac.cnr.it (L. Palchetti).
URL: http://fts.ifac.cnr.it/ (L. Palchetti).

1350-4495/$ - see front matter © 2007 Elsevier B.V. All rights reserved.
doi:10.1016/j.infrared.2007.06.001

fabricated and used in the REFIR-BreadBoard (REFIR-BB) [5] and the REFIR-Prototype for Applications and Development (REFIR-PAD) [6] prototypes of the FTS. The design and the characterisation of the internal coating is described in Section 2. Section 3 is devoted to the design of the cavity geometry. In Section 4, the fabrication of BB is described, and finally in Section 5, the characterisation of the emission performance is shown.

2. Internal coating

The requirements of low reflectance and high thermal conductance can not be easily met by a single compound cavity, where the specularly reflecting surface is also the supporting mechanical structure. BB cavities are usually made with a composite structure: a metallic case with high thermal conductance, typically with the drawback of high reflectance, and a thin surface coating with high absorbance to reduce the internal reflectance.

The internal cavity can be coated with different materials depending on working temperature and frequency range. Different tests have been performed in order to identify the best choice for the infrared (IR) spectral range with materials compatible with working temperatures in the range of −10 to 120 °C. Table 1 reports the characteristics of the tested coatings.

The characteristics of the fabricated coatings are summarised in the following list.

- Xylan©[1] is a fluoropolymer (PTFE – polytetrafluoroethylene) coating developed for low friction application where mechanical components are operated at high temperature. Xylan 1052 is hard, wear resistant, and stable at over 260 °C. Xylan was deposited after sulfuric oxidation.
- OFROFIX is a black lack produced for painting motor mufflers and therefore is resistant to high temperatures. It is filled with pigments to increase blackness and thermal conductivity.
- CAPEC is a nitro matt black lack for automotive applications. It is filled with pigments to increase blackness and thermal conductivity.
- Oxidised copper is obtained by anodic deposition and sulfuric oxidation. Black organic pigments are used to increase surface blackness.

All coatings are grown on Anticorodal 6082 T6 aluminium alloy.

Coating reflectances were measured in the 400–4000 cm^{-1} spectral range with 2 cm^{-1} resolution by using a Nicolet™ FTIR spectrometer. The measurements were performed with the probing beam incident at 4° on the sample surface. Fig. 1 shows the results for the samples reported in Table 1.

[1] www.whitfordww.com.

Table 1
Tested coatings

Coating	Thickness (μm)	Max temperature (°C)
Xylan® 1052	25	285
CAPEC lack	–	–
CAPEC lack with pigments[a]	–	–
OFROFIX lack with pigments[b]	–	300
Oxidised copper	15–20	–
Copper	15–20	–

[a] 22% smoke black, 11% silver graphite, 5% oxide black.
[b] 8% smoke black, 8% silver graphite, 8% oxide black.

Good performances (i.e. a reflectivity less than 10%) in this spectral range are obtained with the Xylan family, the oxidised copper, and the OFROFIX mixture coatings, which also allow the usage at high temperature.

Scattering is not considered in this analysis since surface in all the samples appears to be quite smooth. In the IR range the effect is further enhanced by the longer wavelengths.

3. Cavity geometry

The geometry of the cavity has to be designed in order to maximise the whole BB absorbance, which depends on both the internal surface reflectance and the number of reflections. The surface reflectance depends on the material, as seen in Section 2, and it can be minimised by selecting the proper coating for the spectral interval of interest. The maximisation of the number of reflections is instead dependent on the cavity geometry and the field-of-view (FOV) of the instrument observing the cavity itself.

General treatments have been developed in different ways and under different conditions, see for instance Ref. [7]. Here we present a simple approach, which is able to identity a few geometric parameters that can be optimised for different characteristics of the FOV required by the instrumentation, where the BB sources has to be used. In this analysis we limited our description to the output characteristics required for the BB sources used in the REFIR prototypes, i.e. one source to be used in a collimated beam and another one is to be used in a focused beam.

3.1. Case of a collimated beam

In this case, the optical beam is collimated and therefore is generally quite large. The BB source has usually a size where the diameter D and the length L have more or less the same value. This is the case of the REFIR internal reference BB (RBB), where $D = 64$ mm and $L = 90$ mm. Because of the reduced length, the shape of the internal bottom surface is chosen to be a reversed cone with the tip toward the output aperture, while the lateral surface is a cylinder, Fig. 2.

The number of internal reflections can be calculated by the ray tracing for two particular cases, a near-lateral beam

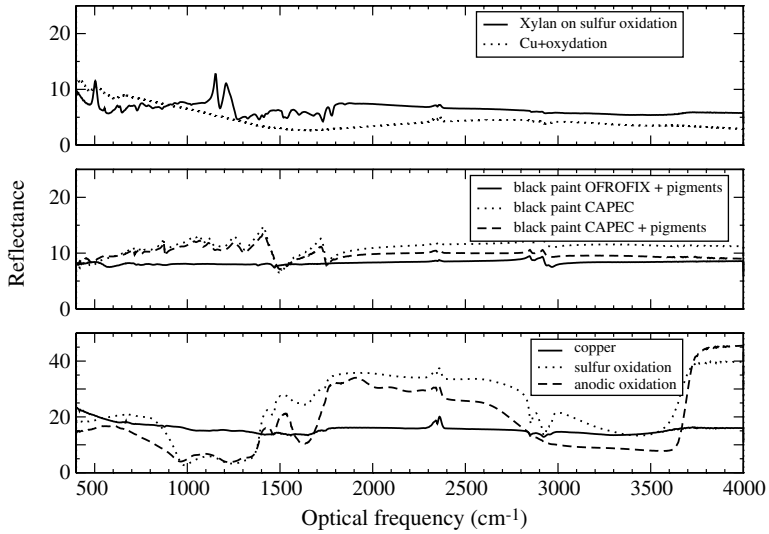

Fig. 1. Reflectance at 4° incident angles measured on the different samples described in the text.

(LB, continuous line), and a near-central beam (CB, dashed line). For the LB, the first and third reflection points are on the bottom surface whereas the other reflection points are on the lateral surface. In the limit of a LB coincident with the vertex, r_N is maximum and it is given by

$$r_N = D(N-3)\tan\left(4\alpha - \frac{\pi}{2}\right), \quad \text{for } N \geqslant 4. \tag{1}$$

For the CB, the first reflection is on the bottom surface whereas the following reflections are on the lateral surface. The distance r_N from the internal bottom to the Nth reflection point along the lateral surface is given by the equation

$$r_N = \frac{D}{2}\tan\alpha + \frac{D}{2\tan 2\alpha} + (N-2)\frac{D}{\tan 2\alpha}, \quad \text{for } N \geqslant 2, \tag{2}$$

where D is the distance of the beam from the lateral surface, and α is the angle at the base of the internal cone.

These results have been used to calculate in these two particular case the number of reflections as a function of the base angle α. In the other cases, when the beam is located between LB and CB, the number of internal reflections is always larger. The results are shown in Fig. 3 for the distance r normalised with respect to the diameter D for the three first reflection points over the lateral surface for $N = 4,5,6$ in the case the LB (continuous line) and for $N = 2,3,4$ in the case of CB (dashed lines). The Figure shows that for a cavity aspect ratio $L/D \geqslant 1.4$, as occurs for RBB, there are at least four internal reflection points when α is about 35 °.

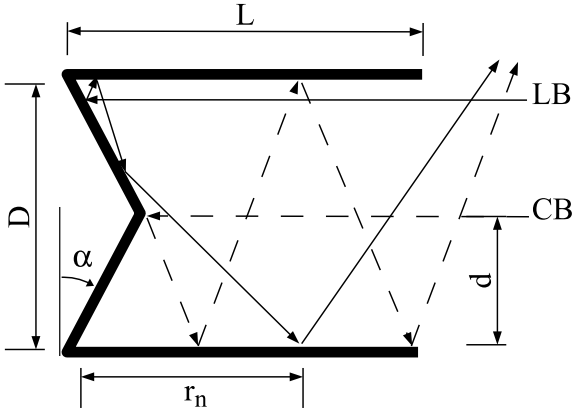

Fig. 2. Internal cavity geometry for the RBB used for collimated beams.

3.2. Case of a focused beam

In this case, the optical beam is focused at the output of the BB cavity. The BB aperture D is therefore smaller and L can be generally larger than $2-3$ D. This is the case of the REFIR internal cold and hot BBs (CBB and HBB, respectively), where $D = 22$ mm and $L = 55$ mm. Because of the greater length, the shape of the internal bottom surface is chosen to be a cone with the tip toward the bottom, while the lateral surface is a cylinder, see Fig. 4. Also in this case, the number of reflections can be calculated by ray tracing for the beams CB and LB.

Let us take the beam aperture equal to $2i$, then LB forms with horizontal axis of the cavity an angle equal to i. LB reflects from the bottom to the lateral surface and the distance r_N from the bottom to the Nth reflection point is

$$r_N = D(N-1)\frac{1+\frac{2L\tan(i)}{D}}{\tan(2\alpha - i)} \quad \text{for } N \geqslant 2. \tag{3}$$

For the CB, the worst condition is when the beam is incident on the cone tip with an angle equal to i. In this case, r_N is given by the equation

$$r_N = D\left(1+\frac{2L\tan(i)}{D}\right)\left[\frac{\frac{5}{2}-N}{\tan(4\alpha+i)} - \frac{\tan\alpha}{2}\right] \quad \text{for } N \geqslant 3. \tag{4}$$

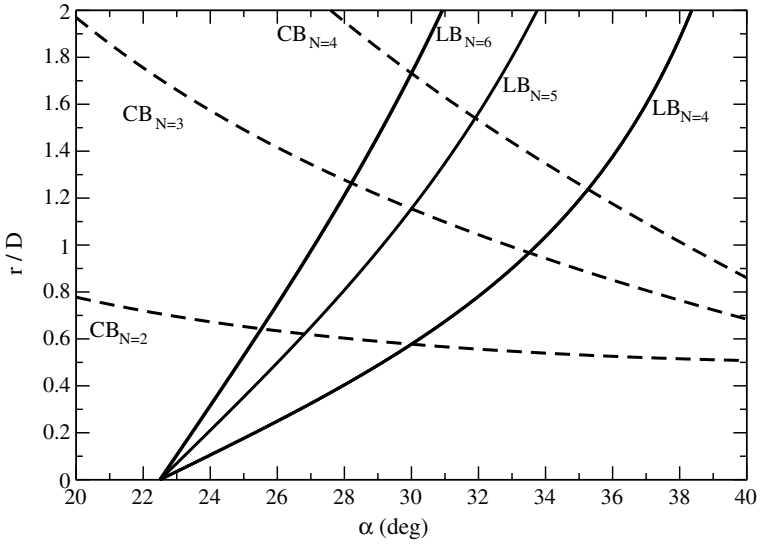

Fig. 3. Normalised distance r/D for a different number N of internal reflections in the case of LB (continuous line), and CB (dashed lines) for RBB geometry.

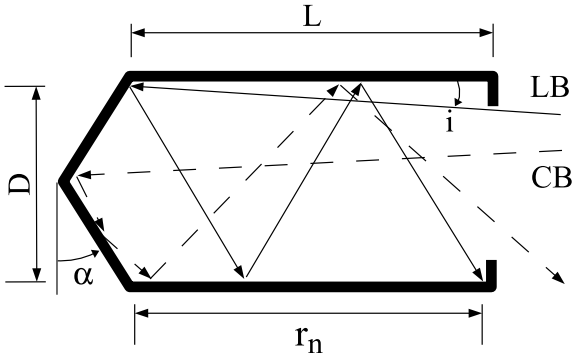

Fig. 4. Internal cavity geometry for the HBB/CBB used for focused beams. LB and CB form with the cavity horizontal axis an angle equal to i.

Fig. 5 shows the results for three reflections on the lateral surface for $N = 3,4,5$ in the both cases. With a cavity aspect ratio $L/D = 2.5$, as in the case of HBB/CBB, there are four internal reflections when α is about 33°.

4. Fabrication and characterisation

Both BB types described in the previous section were used on-board the REFIR prototypes. The type for collimated beams was used as reference for the second input port (RBB), and the smaller type for focused beams as the hot and cold calibration sources (HBB and CBB). The mechanical layout is shown in Fig. 6 and meets the requirements established in the previous Section for a number of internal reflections $\geqslant 4$.

The BB cavities are made by two aluminium pieces, as shown in Fig. 7 in the case of the HBB/CBB type (the collimated beam type is similar): a bottom part (Bp) and a cylindrical shield (Cs). The assembly of these two parts is fixed to an aluminium support (Sp) using a Peltier element (Pe)[2] as a spacer and plastic screws. A resistive heater (Ht)[3] is wrapped around the BB allowing high-temperature operation if needed. Stabilisation near room temperature is achieved through the Peltier element. The source is wrapped in a multilayer insulating sheet and enclosed in a double cylindrical casing (Ca) composed by an internal aluminium shield and an external insulating PTFE sheath.

Four temperature sensors are embedded in the blackbody source, a NTC thermistor (10 kΩ at 25 °C) is used for active stabilisation of the source temperature, and three PT100 resistors for accurate temperature measurement. The position of the PT100 elements, one in the centre and one in the side of the bottom part Bp (PT1 and PT2 in Fig. 6) and one in the front edge of the cylindrical shield Cs (PT3 in Fig. 6), is selected to identify all kind of temperature gradients in the BB.

A single electronic board has been designed to perform both active temperature stabilisation through the Peltier element and the NTC thermistor, and temperature measurement through the three PT100.

4.1. Temperature gradient in the BB coating

The real internal surface temperature of the BB coating can be slightly different from the values measured by PT100 sensors located in the mechanical structure. The temperature gradient ΔT inside the coating can be estimated by making equal the output energy flux, which depends on the BB aperture surface S, the ambient temperature T_a,

[2] Melcor CP 1.0-127-05L.
[3] Minco Flexible Thermofoil™.

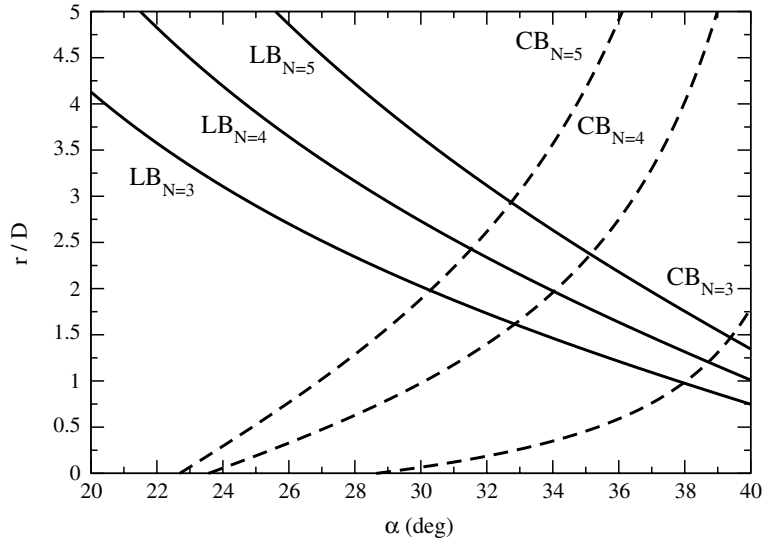

Fig. 5. Normalised distance r/D for a number N of internal reflections in the case of LB (continuous line), and CB (dashed lines) for HBB/CBB sources.

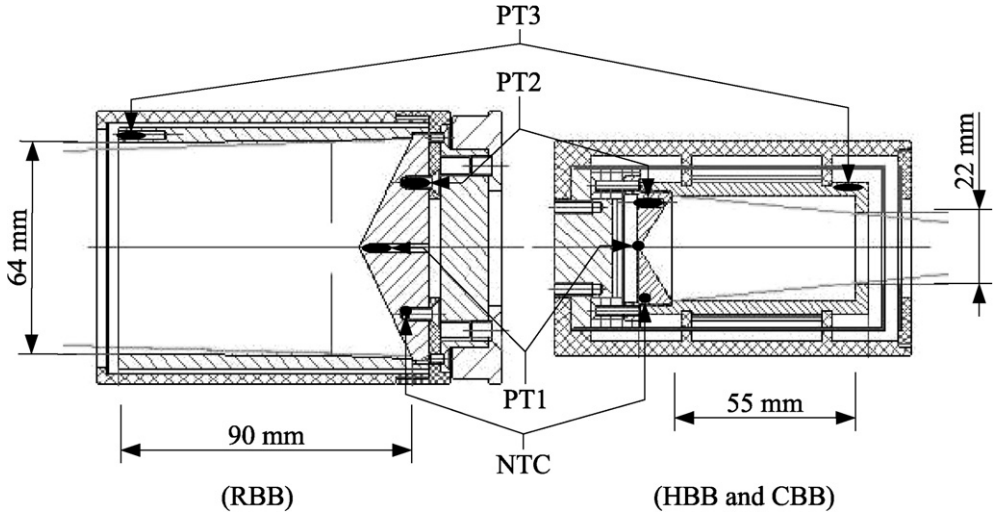

Fig. 6. Mechanical layout for the REFIR RBB (left side) and HBB or CBB (right side). PT1–3 are PT100 temperature sensors, and NTC is a 10 kΩ thermistor.

and the cavity temperature T_{BB}, with the energy transport through the coating internal surface S_i. It is found [8]

$$\Delta T = \sigma_{SB} \frac{S}{S_i} \frac{d}{k} (T_a^4 - T_{BB}^4), \quad (5)$$

where d and k are, respectively, the thickness and the thermal conductivity of the coating, and σ_{SB} is the Stefan–Boltzmann constant. Eq. (5) is calculated for both RBB and HBB/CBB geometry for the Xylan coating ($d = 25.5$ μm, measured with Tencor Instruments Alpha-Step 200 diamond profilometer and $k = 0.25\ \mathrm{WK^{-1}\,m^{-1}}$, typical value for PTFE). Fig. 8 shows ΔT as a function of the temperature difference between the BB and the environment. The temperature gradient can be neglected since it is less than 0.02 K, even in the worse case of the larger temperature difference between the BB and the external environment.

5. Emission performances

In both types of BB and under different heating or cooling conditions, usually a temperature gradient parallel the BB surfaces has been found. Typically along the lateral walls the gradient (temperature difference between PT2 and PT3) can be as high as 5–10 K, instead the difference inside the bottom BB circular structure (temperature difference between PT1 and PT2) is limited to 1–2 K.

Under these typical working conditions, a very simple model has been considered in order to characterise the BB emission law as a function of the three temperatures. The internal cavity has been divided into three regions, the bottom circular surface, the first half lateral surface closer to the bottom, and the second lateral surface closer to the top BB aperture. Each region is characterised by a

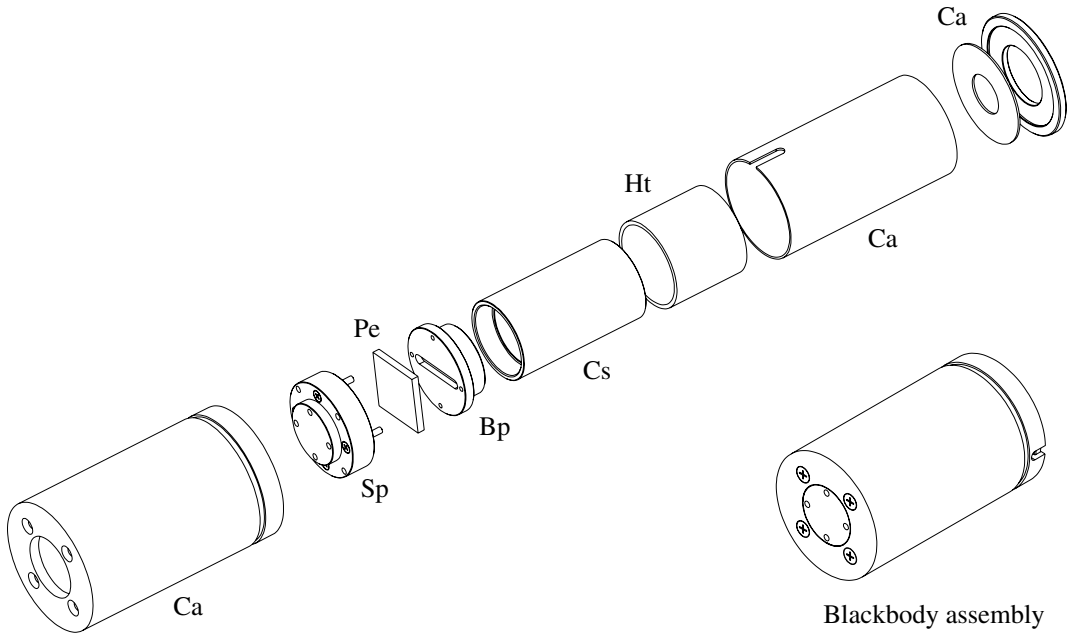

Fig. 7. Exploded view of the blackbody source (focused beam version). Bp: blackbody bottom, Cs: blackbody cylindrical shield, Sp: support, Pe: Peltier element, Ca: external casing, Ht: heater.

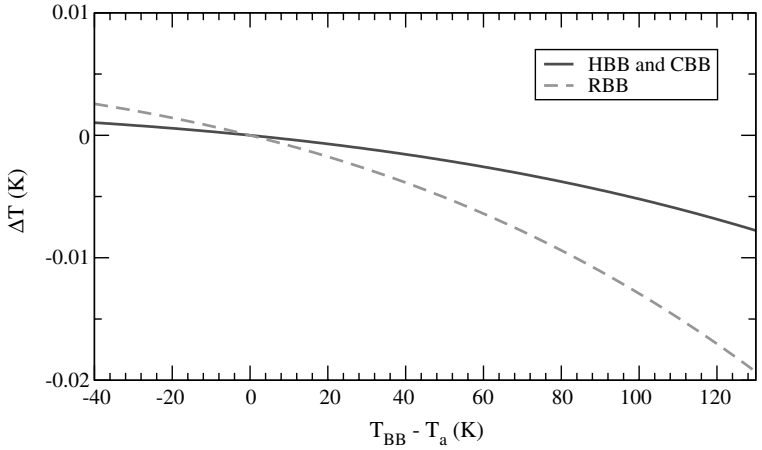

Fig. 8. Temperature gradient ΔT inside the coating as a function of the temperature difference between the BB and the environment. The calculation has been performed with the environment temperature of 20 °C.

single effective temperature, T_{bot}, T_{lat1}, and T_{lat2}, respectively. T_{bot} is given by the average of the temperatures measured in PT1 and PT2. Instead for the lateral surface, a linear gradient between PT2 and PT3 is considered and T_{lat1} and T_{lat2} are taken equal to the average in the two separated regions. The total output emission as a function of optical frequency $L_{\mathrm{BB}}(\sigma)$ is given by adding the emission of these regions considering the possible number of reflections. According to the cavity geometry model described in Section 3, the bottom region emits directly through the output BB aperture and through one reflection, the first lateral region through two reflections, and the second lateral region through three reflections. Therefore $L_{\mathrm{BB}}(\sigma)$ is given by the following equation

$$L_{\mathrm{BB}}(\sigma) = eB(T_{\mathrm{bot}},\sigma) + eRB(T_{\mathrm{bot}},\sigma) + +eR^2B(T_{\mathrm{lat1}},\sigma) + eR^3B(T_{\mathrm{lat2}},\sigma), \quad (6)$$

where R is the coating spectral reflectance, $e = (1 - R)$ is its emissivity, and $B(T,\sigma)$ is the Planck emission function. The first two terms in Eq. (6), which depend essentially only on the temperature of the bottom surface, produce the dominant effect when R is small, as usually occurs in the materials used for the BB internal coating.

Eq. (6) can be used to calculate the emissivity of a BB when the temperature is uniform (i.e. $T_{\mathrm{bot}} = T_{\mathrm{lat1}} = T_{\mathrm{lat2}}$). In the case of a BB coated with Xylan, R can be taken equal to 0.09, which well approximates reflectance, as

Table 2
BB heating laboratory conditions

BB source	PT1 temperature (°C)	PT2 temperature (°C)	PT3 temperature (°C)
HBB	82.9	83.3	91.5
RBB	62.3	62.7	66.3
RBB	14.3	13.7	22.4

shown in Fig. 1, over the whole spectral bandwidth, and Eq. (6) gives an emissivity better than 0.9999.

Eq. (6) can also be used to calculate the brightness temperature (i.e. the effective BB temperature) that can be attributed to the BB emission in the case a temperature gradient inside the BB. The evaluation has been performed in three real conditions measured in laboratory and reported in Table 2. The calculations have been extended down to 100 cm^{-1} by taking $R = 0.09$ also below 400 cm^{-1}, where no measurements are available, and the results are shown in Fig. 9. Fig. 9 also shows that the modeled emission corresponds to a constant BT that is equal to the average of the measurements from the PT1 and PT2 sensors (i.e. the temperature of the bottom surface) within 0.01–0.02 K temperature error in case of a heated source. In the case of a BB temperature near to the ambient the variation of BT with the optical frequency is larger and can reach a few degrees.

To verify this model, an independent measurement of BT has been performed by the IR camera Probeye® TVS 2000, which is sensible to the 1852–3333 cm^{-1} (3–5.4 μm) spectral range. The thermal images of the BB aperture emission are shown in Fig. 10 for the three heating conditions reported in Table 2.

The images show a very uniform temperature field that can be evidenced through a plot of the vertical and horizontal profiles as shown in Fig. 11 for HBB, and in Fig. 12 for RBB heated (top panel) and cooled (bottom panel). When the instrument FOV is inside the central area, i.e. when the beam diameter is smaller than 20 mm for HBB and 60 mm for RBB (as occurs in REFIR-PAD), the BB emission has a constant BT within 0.1 °C.

The BT measured with the IR camera can also be compared with the model estimation given by Eq. (6) and calculated for the same heating conditions. From Fig. 9 we obtain the average of BT in the IR camera spectral range, 83.11 °C for HBB heating condition, 62.51 °C for RBB

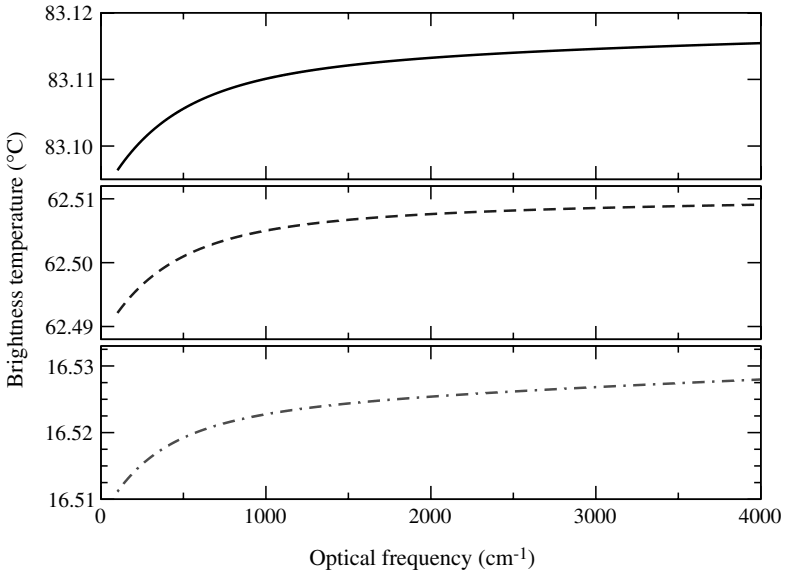

Fig. 9. Brightness temperature calculated from Eq. (6) as a function of optical frequency in three heating conditions, typically used for RBB and HBB.

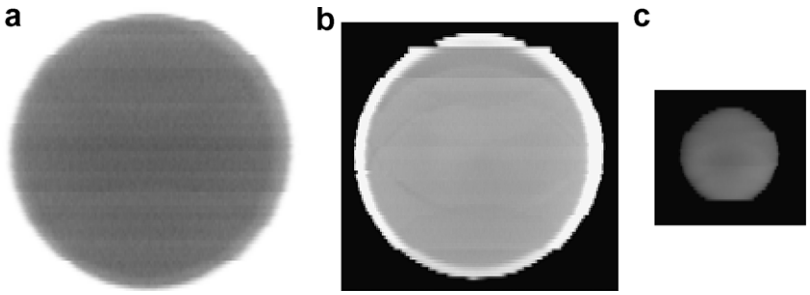

Fig. 10. Thermal images for (a) RBB at about 14 °C, (b) RBB at about 63 °C, and (c) HBB at about 83 °C.

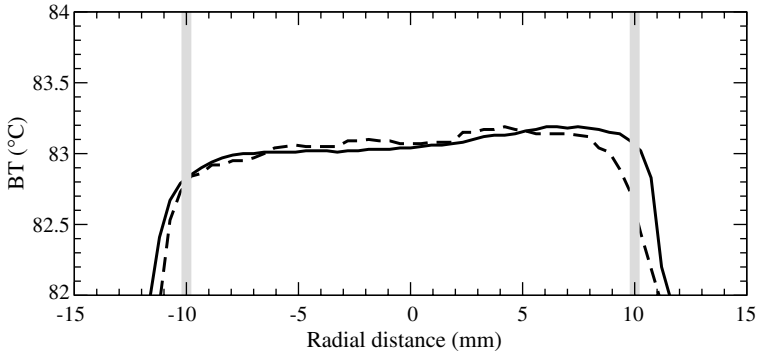

Fig. 11. BT profiles vertical (dashed line) and horizontal (continuous line) for HBB at the measured PT100 temperature of about 83 °C. The REFIR-PAD IFOV is shown by the vertical grey lines.

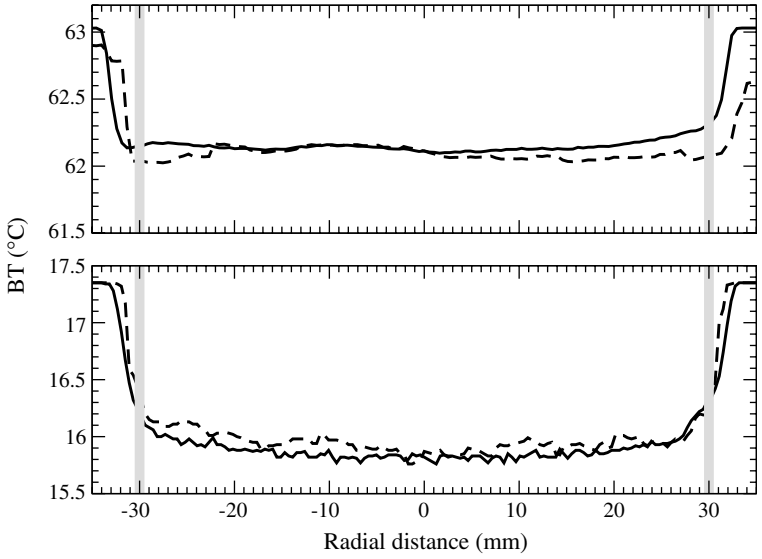

Fig. 12. BT profiles vertical (dashed line) and horizontal (continuous line) for RBB at the measured PT100 temperature of about 63 °C (top panel), and for RBB of about 14 °C (bottom panel). The REFIR-PAD IFOV is shown by the vertical grey lines.

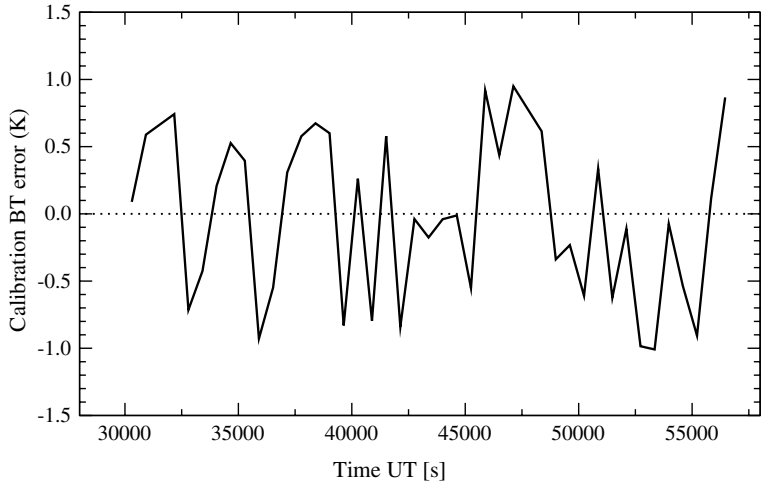

Fig. 13. Calibration BT error measured with REFIR-PAD during the stratospheric flight performed in June 2005 from Brazil [9].

heated, and 16.53 °C for RBB cooled. These values are very close to the IR camera measurements, shown in Figs. 11 and 12, and allow to verify the model with a 0.5 K precision.

These two kind of BB sources were used for on-board calibration of REFIR-PAD for the spectral measurement of the outgoing atmospheric emission during a stratospheric balloon flight [9]. The flight, performed from Brazil near Teresina (5° 5' S, 42° 52' W) on June 30th, 2005, reached the float altitude of 34 km for 8 h. At this altitude, the atmosphere above the instrument is almost transparent at those spectral frequencies where no emission lines of the residual gasses are present. These spectral intervals can be used to evaluate the calibration error by measuring the radiance error with respect to the zero emission of the deep sky observation. The result measured during the flight is shown in Fig. 13, where the radiance error has been converted to brightness temperature error with respect to a reference temperature of 280 K.

The oscillations are within ± 1 K peak-to-peak with a small bias (the average error is about -0.04 K). This result indicates a good calibration performance obtained during field operation of the instrument. The calibration error is also compatible with the laboratory uncertainty, shown previously (Figs. 11 and 12), of the BB source emission.

6. Conclusions

In this paper a detailed description of two kinds of blackbody reference sources and the characterisation of their performance is presented. The sources here described are not intended as state-of-the art devices for ultimate precision, but as high-accuracy systems that can be used as a transfer standard between laboratory characterisations and field-based measurements, for which the use of an absolute standard is not feasible due to requirements of size, weight and operating environment.

Thanks to a simple mathematical model, and extensive laboratory characterisation measurements, the accuracy that can be achieved with an absolute and precise standard reference can be transferred to the field measurements with only a little increase of computational load. The emission characteristics of the fabricated sources are measured both in laboratory and in field operations with the REFIR-PAD FTS instrument. The emission turns out to be known with an emissivity better than 0.9999 and a temperature error of about 0.5 K.

Acknowledgements

The authors wish to thank their colleagues of IFAC-CNR, Dr. M. Picollo and Mr. B. Radicati, for the spectral measurements of the surface reflectances, and Mr. I. Pippi for the measurements performed with the IR camera.

References

[1] J.B. Fowler, A 3rd-generation water bath based blackbody source, J. Res. Natl. Inst. Stand. 100 (1995) 591–599.
[2] I.M. Mason, P.H. Sheather, J.A. Bowles, G. Davies, Blackbody calibration sources of high accuracy for a spacebourne infrared instrument: the along track scanning radiometer, Appl. Opt. 35 (1996) 629–639.
[3] V.I. Sapritsky, B.B. Khlevnoy, V.B. Khromchenko, B.E. Lisiansky, S.N. Mekhontsev, U.A. Melenevsky, S.P. Morozova, A.V. Prokhorov, L.N. Samoilov, V.I. Shapoval, K.A. Sudarev, M.F. Zelener, Precision blackbody sources for radiometric standards, Appl. Opt. 36 (1997) 5403–5408.
[4] R. Rizzi, L. Palchetti, B. Carli, R. Bonsignori, J.E. Harries, J. Leotin, S. Peskett, C. Serio, A. Sutera, Feasibility study of the space-borne Radiation Explorer in the Far InfraRed (REFIR), in: A.M. Larar, M.G. Mlynczak (Eds.), Optical Spectroscopic Techniques, Remote Sensing and Instrumentation for Atmospheric and Space Research IV, Proceedings of SPIE, vol. 4485, 2002, pp. 202–209.
[5] L. Palchetti, G. Bianchini, F. Castagnoli, B. Carli, C. Serio, F. Esposito, V. Cuomo, R. Rizzi, T. Maestri, Breadboard of a Fourier transform spectrometer for the radiation explorer in the far infrared atmospheric mission, Appl. Opt. 44 (2005) 2870–2878.
[6] G. Bianchini, L. Palchetti, B. Carli, A wide-band nadir-sounding spectroradiometer for the characterization of the Earth's outgoing long-wave radiation, in: R. Meynart, S.P. Neeck, H. Shimoda (Eds.), Sensors, Systems, and Next-Generation Satellites XII, Proceedings of SPIE, vol. 6391, 2006, p. 63610A.
[7] Z. Chu, R.E. Bedford, W. Xu, X. Liu, General formulation for the intergrated effective emissivity of any axisymmetric diffuse blackbody cavity, Appl. Opt. 28 (1989) 1826–1829.
[8] B. Carli, Design of a blackbody reference standard for submillimeter region, IEEE Trans. Microwave Theory Tech. MTT-22 (1974) 1094–1099.
[9] L. Palchetti, C. Belotti, G. Bianchini, F. Castagnoli, B. Carli, U. Cortesi, M. Pellegrini, C. Camy-Peyret, P. Jeseck, Y. Té, Technical note: first spectral measurement of the Earth's upwelling emission using an uncooled wideband Fourier transform spectrometer, Atmos. Chem. Phys. 6 (2006) 5025–5030.